

# Combined magnetic resonance imaging approach for the assessment of in vivo knee joint kinematics under full weight-bearing conditions

Proc IMechE Part H:  
*J Engineering in Medicine*  
 2015, Vol. 229(6) 439–451  
 © IMechE 2015  
 Reprints and permissions:  
[sagepub.co.uk/journalsPermissions.nav](http://sagepub.co.uk/journalsPermissions.nav)  
 DOI: 10.1177/0954411915585863  
[pih.sagepub.com](http://pih.sagepub.com)  


**Ghaith Al Hares<sup>1</sup>, Jörg Eschweiler<sup>1,2</sup> and Klaus Radermacher<sup>1</sup>**

## Abstract

The development of detailed and specific knowledge on the biomechanical behavior of loaded knee structures has received increased attention in recent years. Stress magnetic resonance imaging techniques have been introduced in previous work to study knee kinematics under load conditions. Previous studies captured the knee movement either in atypical loading supine positions, or in upright positions with help of inclined supporting backrests being insufficient for movement capture under full-body weight-bearing conditions. In this work, we used a combined magnetic resonance imaging approach for measurement and assessment in knee kinematics under full-body weight-bearing in single legged stance. The proposed method is based on registration of high-resolution static magnetic resonance imaging data acquired in supine position with low-resolution data, quasi-static upright-magnetic resonance imaging data acquired in loaded positions for different degrees of knee flexion. The proposed method was applied for the measurement of tibiofemoral kinematics in 10 healthy volunteers. The combined magnetic resonance imaging approach allows the non-invasive measurement of knee kinematics in single legged stance and under physiological loading conditions. We believe that this method can provide enhanced understanding of the loaded knee kinematics.

## Keywords

Kinematics, total knee replacement, magnetic resonance imaging, weight-bearing, total knee arthroplasty

Date received: 3 June 2014; accepted: 15 April 2015

## Introduction

An accurate in vivo measurement of knee joint motion under physiological weight-bearing conditions is necessary to understand the natural motion behavior of the knee joint. Besides the understanding of the physiological knee motion, the acquisition in specific functional information is of special importance in osteoarthritis (OA) cases, where OA symptoms (e.g. pain) are dependent on specific movement and weight-bearing patterns. The total knee arthroplasty (TKA) is ranked on position 20 of the 50 most performed surgical interventions in Germany with more than 154,792 TKAs performed every year.<sup>1</sup> The restoration in physiological loading conditions and knee biomechanics is the major aim of this procedure and has received more attention in recent years. One of the most critical biomechanical aspects involved in the workflow of present TKA strategies is the intraoperative optimization of ligament balancing.<sup>2</sup> The medial-lateral ligament balancing is

usually performed with passive flexion-extension in unloaded situations. A recent *in vitro* biomechanical study<sup>2</sup> showed considerable difference in medial and lateral ligament strains after TKA during loaded flexion compared to unloaded passive flexion. The outcome of this study confirms that the quality of such passive unloaded ligament balancing is questionable and, therefore, emphasizes the need of detailed and specific knowledge on the biomechanical behavior of loaded knee structures.

<sup>1</sup>Helmholtz-Institute for Biomedical Engineering of the RWTH Aachen University, Aachen, Germany

<sup>2</sup>Department for Orthopedic Surgery, University Hospital Aachen, Aachen, Germany

## Corresponding author:

Ghaith Al Hares, Helmholtz-Institute for Biomedical Engineering of the RWTH Aachen University, Pauwelsstr. 20, 52074 Aachen, Germany.  
 Email: [alhares@hia.rwth-aachen.de](mailto:alhares@hia.rwth-aachen.de)

## ***State-of-the-art on magnetic resonance imaging-based methods for the assessment of knee kinematics***

Conventional knee magnetic resonance imaging (MRI) is normally performed in supine position and under non-weight-bearing conditions. Several studies have evaluated joint kinematics using stress MRI techniques<sup>3–9</sup> and reported that evaluating a patient in non-weight-bearing position alone may lead to misdiagnoses.<sup>10–13</sup> These techniques have been used to evaluate knee kinematics and its change due to anterior cruciate ligament (ACL) lesions or after ACL reconstruction procedures<sup>14–18</sup> and to evaluate the meniscus biomechanics during knee flexion/extension.<sup>19,20</sup> In a previous work, Fellows et al.<sup>21</sup> have reported very promising high accuracy and subject repeatability of dynamic MRI under specific loading conditions based on a registration of high-resolution static MRI data to low-resolution dynamic MRI data in three subjects. A similar method is reported in recent work by D'Entremont et al.<sup>9</sup> The limitation of the work by Fellows et al. and D'Entremont et al. lies in that in both studies the stress MRI measurements were acquired in supine and not in upright positions.

Due to the higher availability of closed-bore scanners compared to upright open-bore scanners, they have been commonly used with customized harness and footplates as a supine alternative to upright weight-bearing measurements.<sup>22</sup>

In closed-bore scanner scenarios, the use of a harness and footplate is normally necessary to simulate the weight-bearing knee movements. In this option, the movement capture is usually performed in atypical loading positions where the subject is laying in supine positions either with help of back support or directly on scanner table. Regarding knee kinematics, physiological upright weight-bearing conditions (e.g. standing and walking) could, however, not be fully considered in such measurements as the influence of gravitational forces—involved in physiological cases—is not considered here and range of knee flexion is usually limited by the size of scanner bore. The cine phase contrast (cine PC) MRI techniques, which were originally developed for the acquisition of a beating heart, have also been adapted for imaging musculoskeletal tissue during motion<sup>23,24</sup> and were used to evaluate tendon strain<sup>25,26</sup> and joint kinematics.<sup>15,27,28</sup> The major drawback in cine PC MRI is the need for multiple repetition of the same motion cycle to ensure good measurement quality and it involves, therefore, the usage of motion guiding devices to limit undesirable out-of-plane motions in the tracked object. The use of these external devices often involves the application of undesired non-physiologic forces on the musculoskeletal structure of interest, which may quickly alter the real “physiological” motion.<sup>29</sup> Another challenging issue in this technique is the selection of the imaging plane. Large amounts of out-of-plane motion can cause additional error when

computing tissue displacements from the velocity data and can critically compromise the measurement quality.<sup>29,30</sup> The potential of real-time MRI originally developed for heart motion and blood flow imaging—for imaging musculoskeletal tissue during motion has been shown in previous studies.<sup>31–33</sup> Tibiofemoral and patellofemoral kinematics and the change of moment arms during knee motion have been also investigated in previous using weight-bearing real-time MRI.<sup>13,34–36</sup> A review on the cine PC MRI and real-time MRI techniques can be found in a recent review paper by Shapiro and Gold.<sup>22</sup>

### ***Limitations of the state-of-art methods***

***Loading conditions.*** A general disadvantage of state-of-art approaches is the movement capture in atypical loading positions with no full consideration of physiological upright weight-bearing conditions and limited flexion range. Although, more physiological loading has been achieved using upright open-bore MRI<sup>17,37</sup> subjects were usually standing with the help of a supporting backrest. Since current upright scanners prevent full vertical position, backrests must usually be inclined backwards to ensure comfortable stance during image acquisition. However, it is questionable to what extent the body weight is supported by the backrest. In two recent studies, Besier et al.<sup>38,39</sup> stated that ~90% of body weight is supported during the scan. Moreover, joint scans are most often performed in bipedal stance, which is inadequate for studying physiological knee loading in other situations where the body weight is completely transferred onto one leg, for example, during the stance phase in walking or stair climbing. To our knowledge, there is no previously published work on capturing knee kinematics in single legged stance and under physiological full weight-bearing.

***Mechanical leg axis and alignment.*** However, previous MRI-based methods for the *in vivo* measurement of knee kinematics had focused on the movement capture of the loaded flexion/extension without further considerations of the mechanical leg axis. The information on the mechanical leg axis is of special importance when investigating kinematic quantities that are influenced by the leg alignment prior to recording kinematics (i.e. varus/valgus leg deformities or misalignment may influence the abduction/adduction movement). Furthermore, investigations of inter-subject variability concerning joint morphology and morphology-driven kinematics (due subject-specific joint morphology and alignment) should take a priori information on loaded mechanical axis into account. According to our knowledge, none of the previously introduced MRI-based approaches have investigated loaded knee kinematics with a priori *in vivo* information on the mechanical leg axis in the examined subjects.

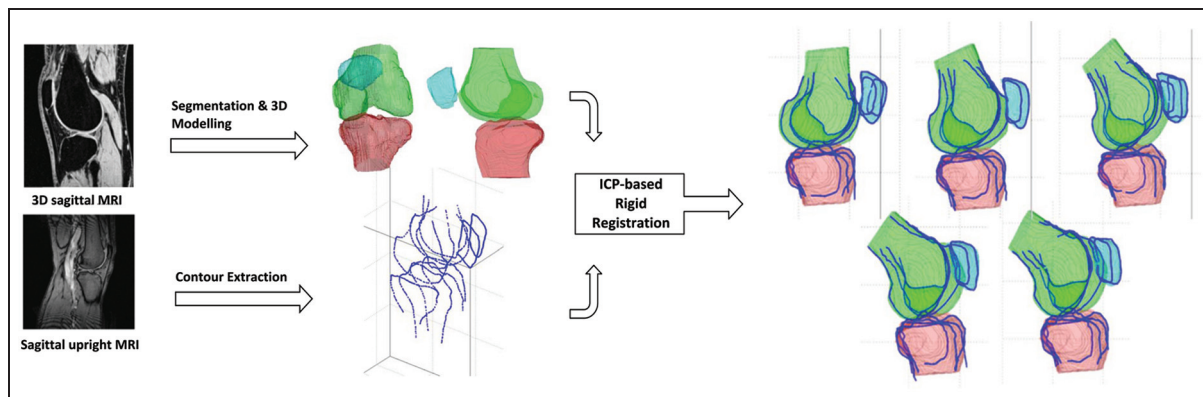


**Figure 1.** Registration method for obtaining knee flexion kinematics in single legged stance under full weight-bearing.

**Table I.** Scan parameters of the MRI techniques used in the kinematic study.

	High-resolution scan	Static upright
Scanner	Philips, Inters, 1.5 T	Upright™ MRI, FONAR, 0.6 T
MRI sequence	3D FS T1-FFE	2D steady state GE
Scan planes	Sagittal	Sagittal
TR (ms)	60	143
TE (ms)	5	17
Flip angle (°)	40	30
Pixel spacing (mm)	0.27 × 0.27	0.54 × 0.54
Slice thickness (mm)	3	4
Slice gap (mm)	1.5	15
Matrix	512 × 512	480 × 480
FOV (mm)	140	259
Scan time (min)	< 15	< 27

MRI: magnetic resonance imaging; 3D: three-dimensional; 2D: two-dimensional; TR: repetition time; TE: echo time; FOV: field of view.

In this work, we propose a combined MRI approach, which allows the measurement of the mechanical leg axis and the assessment of knee kinematics under physiological loading conditions in single legged stance.

## Material and methods

The tibiofemoral kinematic measurement method relies on registering bone models obtained from a high-resolution MRI scan to loaded bone positions (bony outlines) derived from fast, low-resolution upright-MRI scans (Figure 1).

### MRI

High-resolution three-dimensional MRI datasets (sagittal fat-suppressed T1-weighted fast field echo images (FS T1-FFE)) of the knee joint were obtained from 10 healthy volunteers (all are males, age range: 30–55 years, body length range: 1.68–1.91 m) in supine position using a 1.5-T Philips-Intera scanner to derive detailed subject-specific anatomical information (Table 1).

In a second step, full weight-bearing image data were acquired using a 0.6-T, full-body upright-MRI system

(Upright™ MRI, FONAR Corporation, Melville, NY, USA), Figure 2.

The upright-MRI acquisition consists of multi-two-dimensional static sagittal scans in the knee joint at pre-defined flexion positions. Table 1 includes the parameters of the developed upright-magnetic resonance (MR) scan. Sample upright MR images obtained during loaded flexion are illustrated in Figure 2. We used sagittal plane images because of their advantage to capture the three joint components (femur, tibia and patella) simultaneously. Each sagittal scan consists of four slices where two slices were planned to cross through the patella to ensure robust three-dimensional position measurement and registration in subsequent steps. Starting with full knee extension, each subject was asked to increase the flexion angle in five steps to reach the maximum flexion angle, which was available under space limitation in the subject's thigh size and knee coil geometry. To reduce the single legged upright standing time and related muscular tension and fatigue, additional external measurement and control of the flexion angles was not included in this study. The range of the achieved flexion for each subject was obtained during the kinematic calculation based on the convention of the joint coordination system (JCS) proposed by Grood and Suntay.<sup>40</sup> A solenoid receiver coil with a

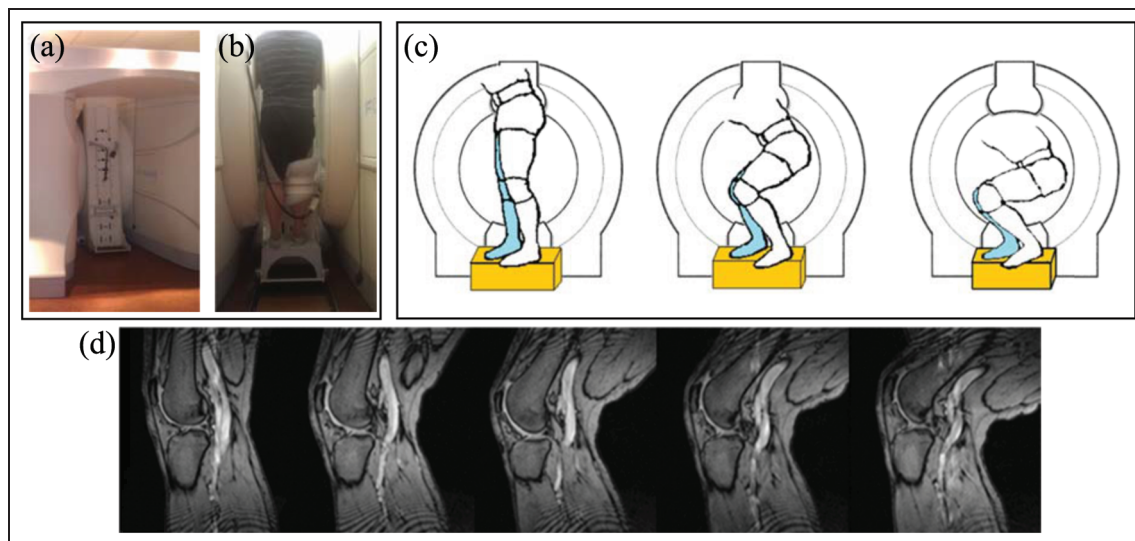


**Figure 2.** (a) The FONAR upright-MRI system used in this study, (b, c) subject positioning and coil setup used in the acquisition of the single legged knee flexion under full weight-bearing and (d) example of the MRI acquisition obtained in single legged stance during the knee flexion.

vertical coil axis perpendicular to the direction of the upright scanner's magnetic field (horizontal direction in our case) was used to ensure optimal signal-to-noise ratios (SNR). The coil setup preserves the optimal right-angle relationship between magnetic field direction and the coil axis during knee flexion. Knees were softly padded for stabilization in lateral-medial direction only in order to reduce motion artifacts. No stabilization in the anterior-posterior direction was applied to ensure unrestricted movement in the flexion plane. With the overall setup, translational motion in the anterior-posterior plane and rotational motion in the axial plane (internal/external rotation) remained, therefore, unconstrained. The inclination of the subject's body in medial-lateral direction was highly restricted by the limited width of the magnet opening. During all static flexion acquisitions, the subjects were allowed to lean back on a movable, trans-polar stabilization bar positioned behind the subject in the scanner gap. The purpose of this bar was to prevent falling backwards during the flexion acquisition. Before each flexion angle, the height of the bar was adjusted so that no sitting on it was possible. At each flexion angle, the subjects were asked to transfer their body weight onto the leg being imaged and maintain the pre-defined flexion position in single legged stance while the four sagittal MR slices in the knee were taken. The upright MR sequence was optimized so that a trade-off between image quality and scan time was achieved. The MR acquisition at every flexion angle takes 39 s. The subjects were allowed to rest for 1–2 min between subsequent loading scans. Although all MRI acquisitions were obtained after positioning the subject's knee in the iso-center of the scanner, the image quality at large flexion angles was slightly degraded due to subject's fatigue and increased tremor in surrounding muscles. The acquisition time for the knee flexion was less than

27 min on average including coil setup, reference scans and scan planning.

### Three-dimensional surface mesh preparation

Four (for femur and tibia) and two (for patella) bone outlines were identified for each fully weight-bearing flexion position by segmenting the low-resolution MR images taken during a loading cycle.

Three-dimensional anatomical models for all three knee bones were obtained from manual segmentation of the high-resolution supine MR scans. All manual segmentations involved in this study were obtained by one experienced operator.

An isotropic resampling with linear interpolation was applied to the original three-dimensional models to obtain high-density models for further kinematic measurements. From now on, we call the resulting meshes “the original meshes.” Due to the magnitude of slice thickness in the high-resolution supine MR scans, the anatomical surface models reconstructed from manual segmentation normally show an obvious stepping artifact. In reality, these anatomical surfaces are much more regular and smooth. However, tibiofemoral and patellofemoral kinematic measurements might be affected by the resolution and quality of the three-dimensional meshes used in the registration approach. This is expected, for example, in biomechanical simulation scenarios where the kinematics is driven by the surface of the articulated components (e.g. using the Force Dependent Kinematics (FDK) method<sup>41,42</sup>), or in cases where the estimation of contact area (points) is important (e.g. the recent work of Chen et al.<sup>37</sup>). In our approach, the kinematic analysis relies entirely on the accuracy of the underlying iterative closest points (ICP)-based shape-matching technique (more details on the approach are given in the next section). Although

inaccuracies in the preparation of high-resolution models and low-resolution bony outlines (through, for example, segmentation errors) were expected in each three-dimensional modeling step, we do not anticipate a considerable effect of such inaccuracies on the ICP registration outcomes. The number of surface vertices involved in the ICP registration would rather affects the total registration time for all flexion positions. A three-dimensional model preparation (mesh reduction and smoothing) that ensures a robust registration in an acceptable registration time is, therefore, desirable. To address this, we assessed up to which degree various smoothed and reduced versions of femur, tibia and patella anatomical meshes would affect the registration with loaded flexion images. Six mesh reduction steps were performed on the original meshes of femur, tibia and patella (from one subject) by merging surface vertices within six pre-defined merging distances (0.25, 0.50, 0.75, 1.00, 1.25 and 1.50 mm). Each mesh reduction step was followed by a non-shrinkage smoothing step using the Taubin smoothing algorithm<sup>43</sup> to reduce the stepping and bumping effects. For mesh reduction and smoothing, the implementation of Visual Computing Lab—STI—CNR in MeshLab<sup>44</sup> was used.

### ***Effect of surface mesh preparation on registration results***

Anatomical axes for each bone were defined in the high-resolution MR scans following the convention of the JCS.<sup>40</sup> Because of the reduced field of view in hip and ankle directions (due to the size of the knee coil used), the definition of the long axes of the tibia and femur were modified from the original method to be along the most superior centroid of the femur shaft and to the most inferior centroid of the tibia shaft.

For each knee bone, seven meshes (one original and six reduced and smoothed versions) were included in the kinematic analysis to evaluate the effect of mesh size and smoothness on the registration outcome and kinematic analysis. All seven meshes were registered to each low-resolution loaded flexion from the upright image set using the ICP algorithm.<sup>45</sup> In this step, the three-dimensional high-resolution surface models were registered (shape-matched) to the low-resolution bony outlines describing the position of knee components in loaded knee flexion. Because a successful match of the ICP depends on an accurate first estimation of model position, approximate alignments of high-resolution three-dimensional models to data points were found manually before the shape-matching was performed.

Rotation matrices and translation vectors describing the movement of each three-dimensional model to its registered alignment in the full extension contours (first static acquisition) are recorded and taken as initial conditions for ICP registration between full extension and first flexion acquisition. The same principle was taken to ensure successful ICP registrations between

subsequent flexion acquisitions. The high-resolution three-dimensional models of femur, tibia and patella were separately registered with their corresponding contours in the movement data to allow tracking and kinematic evaluation of individual knee components. Registration steps using reduced and smoothed meshes were evaluated against those obtained with the original meshes. Evaluation was carried out in one subject by comparing calculated transformation parameters (translation and rotation) for all registration steps. In this comparison, the three translation components ( $tx, ty, tz$ ) and four rotation components (axis-angle representation with three axis components ( $ax, ay, az$ ) and one angular component ( $\theta$ )) were used (Figure 3). The mesh preparation (reduction and smoothing) that provides

- Surfaces meshes with acceptable surface deviation from the original meshes,
- Acceptable deviation in registration (in terms of its translation and rotation components) compared to the registration obtained with the original meshes, and
- Acceptable overall registration time was then used for further processing of remaining subject models and subsequent kinematic analysis.

Tibiofemoral kinematics was finally carried out by calculating the translations and rotations for the tibia with respect to the femur using the JCS method.<sup>40</sup> For the kinematic analysis, internal/external rotation, anterior/posterior translation, adduction/abduction and medial/lateral translation were calculated for the tibia with respect to the femur. Figure 4 illustrates the anatomical landmarks used to compute the coordinate systems for femur and tibia.

Data preparation, three-dimensional model construction and registration as well as kinematic analysis were performed using a group of dedicated MATLAB programs (Mathworks Inc., USA).

### ***Mechanical leg axis determination***

For the determination of the mechanical leg axis and lower limb alignment, the centers of femoral head, the knee joint center and ankle joint center are usually identified on a single coronal view.<sup>46,47</sup> As femoral head, knee and ankle could not be obtained on a single coronal MR image, a multi-station imaging protocol was developed including acquisitions around hip, knee and ankle joint (Table 2). For a reliable analysis of the mechanical leg axis and measurement of Hip–Knee–Ankle (HKA)-angle, both coronal and axial slices were acquired around femoral head and neck, knee and ankle joint in a weight-bearing bipedal stance. Axial slices were acquired to allow later torsion measurements and correction of femur and tibia. In contrast to the work presented by Liodakis et al.<sup>48</sup> our setup involves the positioning of three different coils around hip, knee and ankle prior to image acquisition (Figure 5(a)–(d)).

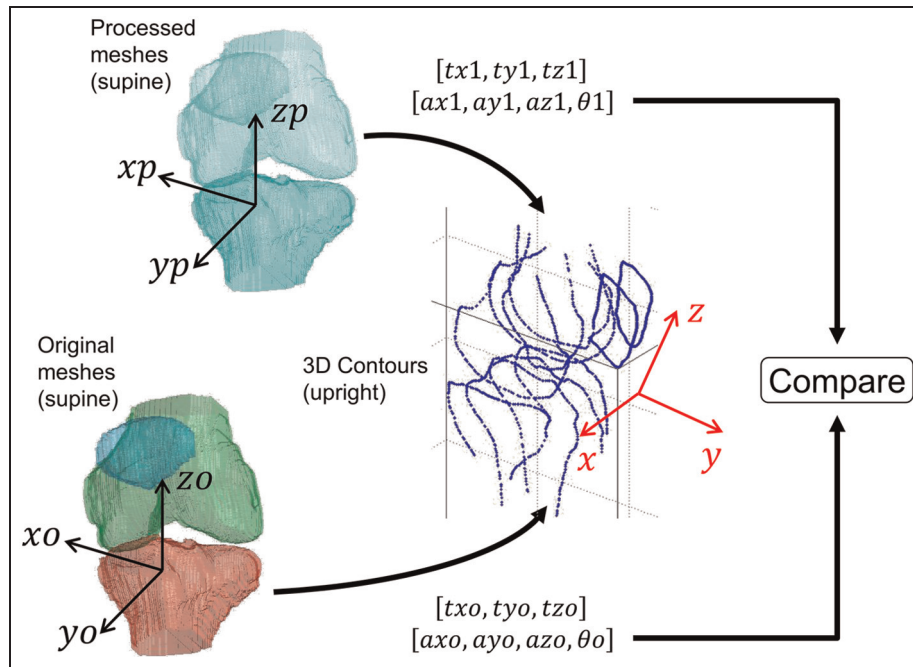


**Figure 3.** Schematic illustration of the evaluation principle of the effect of mesh processing on supine MRI/upright-MRI registration. Registration parameters ( $tx, ty, tz, ax, ay, az, \theta$ ) obtained with each processed mesh (femur, tibia and patella) were compared with those obtained with the original meshes. In the comparison of rotation components, the axis-angle representation was used.

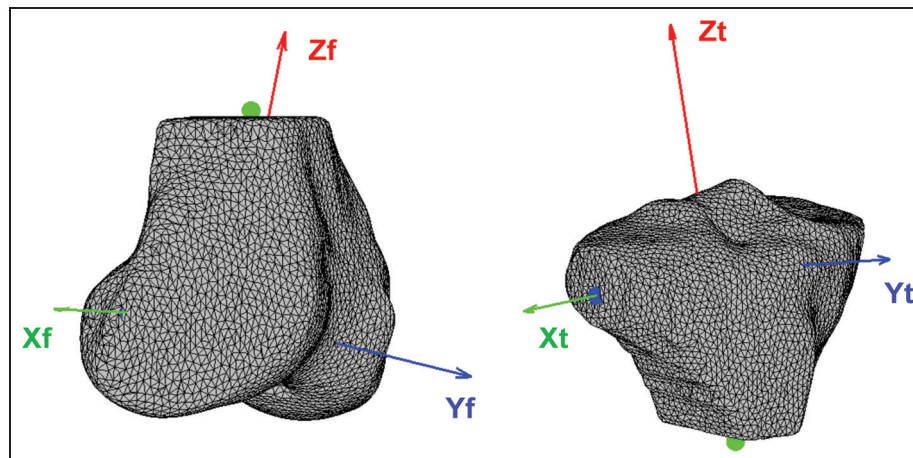


**Figure 4.** The coordinate system for the femur (left) and tibia (right) used in the kinematics calculation.

This has the potential to considerably reduce movement artifacts in contrast to the coil-interchanging approach of Lioudakis et al.<sup>48</sup> As with the flexion acquisition, the SNR was optimized by the right-angle relationship between the axis of the solenoid receiver coils and the horizontal direction of the magnetic field. The image acquisition starts around the hip joint. Knee and ankle acquisitions were subsequently obtained after corresponding adjustments of table elevation. Table elevations for hip, knee and ankle scans were manually chosen and registered to ensure optimal image quality near the magnet iso-center. The acquisition time was less than 22 min on average including coil setup, reference scan and scan planning. A dedicated bi-planar (coronal/axial) image-based approach was developed

for the determination of the three joint centers. The registration between all MR acquisitions was established using information on table elevation and image position and orientation contained in the DICOM header file. After this registration, the centers of femoral head, knee and ankle joints were determined on the coronal view and fine-tuned with help of the orthogonal axial view using a dedicated graphical user interface (Figure 6).

## Results

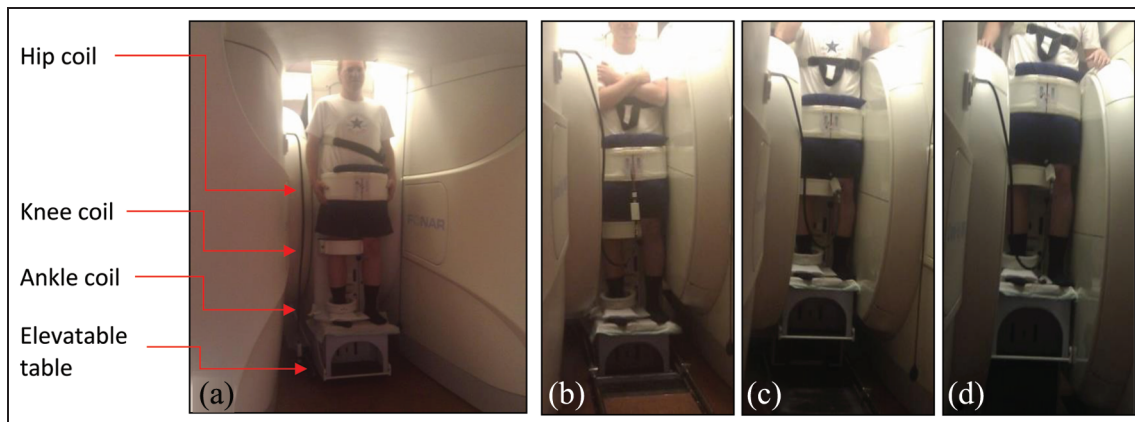
### Effect of surface mesh preparation on registration results

Anatomical surface meshes generated by the proposed mesh preparation procedure are illustrated in

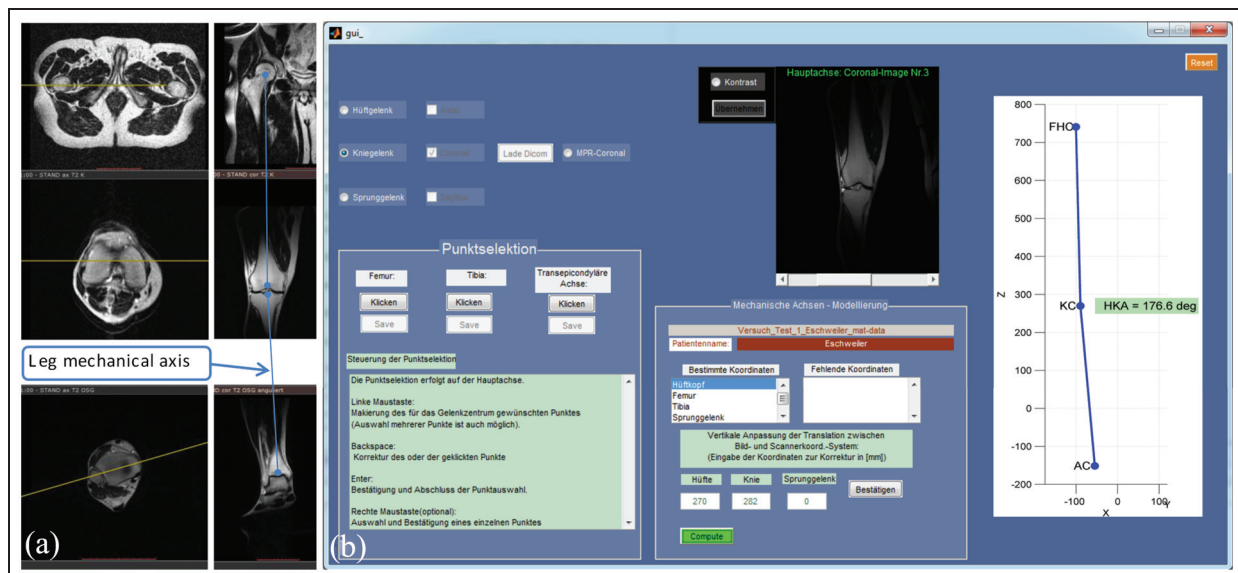
**Table 2.** Scan parameters used in the upright-MRI-based measurement of the mechanical leg axis.

	Hip axial	Hip coronal	Knee axial	Knee coronal	Ankle axial	Ankle coronal
Pulse sequence	T2-FSE	T2 - FSE	T2 - FSE	T2 - FSE	T2-FSE	T2 - FSE
Number of slices	10	7	10	7	7	7
TR (ms)	1645	1603	1645	2300	2300	2300
TE (ms)	160	100	160	160	160	160
Flip angle (°)	90	90	90	90	90	90
Pixel spacing (mm)	$1.56 \times 1.56$	$0.78 \times 0.78$	$0.93 \times 0.93$	$0.78 \times 0.78$	$0.93 \times 0.93$	$1.56 \times 1.56$
Slice thickness (mm)	6	8	6	6	6	7
Slice gap (mm)	9	10	9	7	8	8
Matrix	$256 \times 256$	$512 \times 512$	$256 \times 256$	$512 \times 512$	$256 \times 256$	$256 \times 256$
FOV (mm)	40	40	24	40	24	40
Scan time (s)	79	52	72	55	55	55

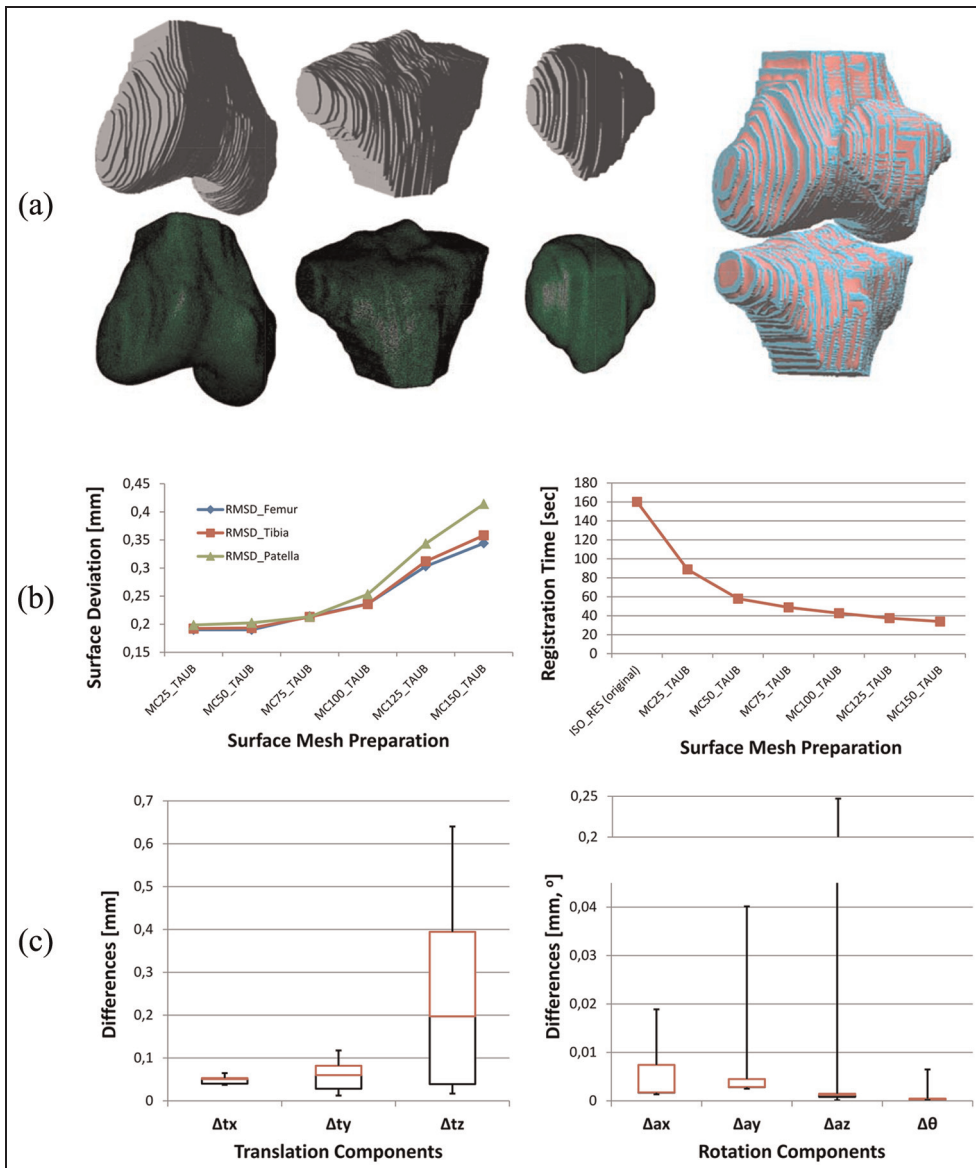
TR: repetition time; TE: echo time; FOV: field of view.



**Figure 5.** (a) Subject positioning and full weight-bearing acquisition with three coil setup and table elevation and (b, c and d) table elevations for hip, knee and ankle acquisitions, respectively.



**Figure 6.** Example on the determination of the mechanical leg axis and the measurement of the Hip–Knee–Ankle angle (HKA) with the proposed upright method: (a) subject-specific bi-planar acquisitions of hip, knee and ankle under full weight-bearing conditions and (b) developed graphical user interface allows for the interactive determination of the axis. FHC, KC and AC denotes the femoral head center, the knee joint center, and the ankle joint center, respectively.



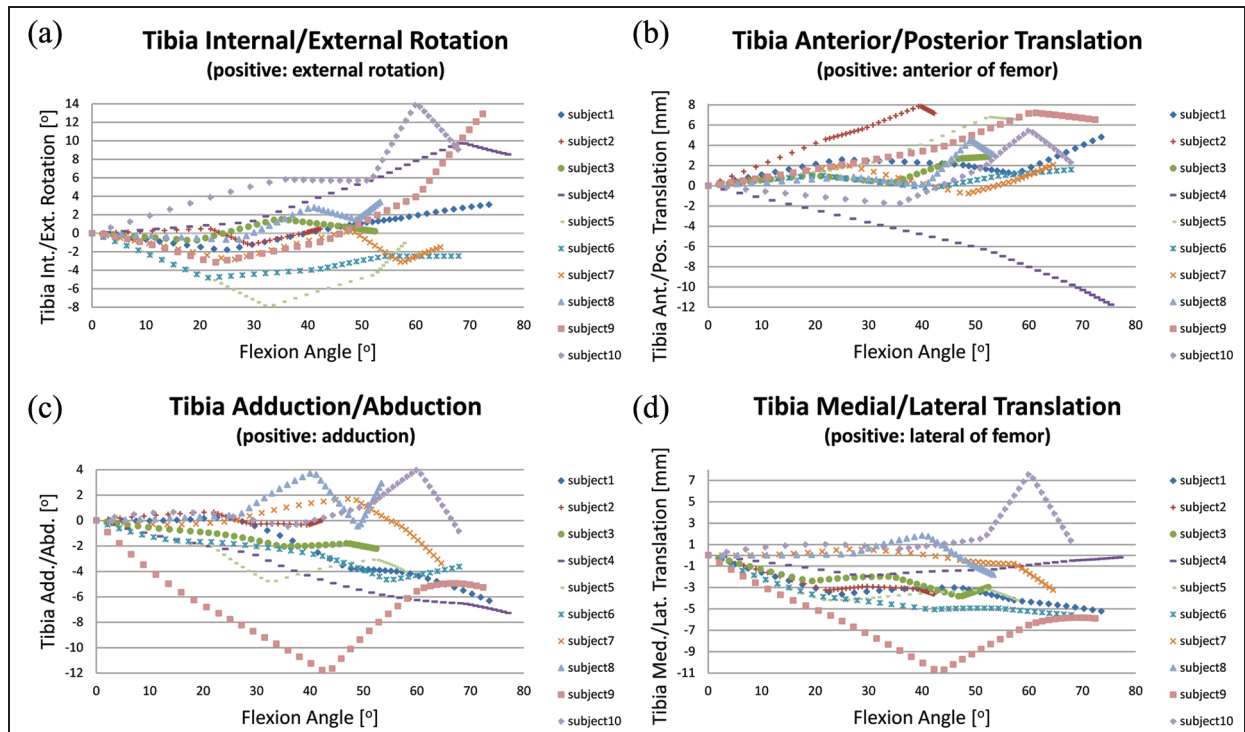
**Figure 7.** Three-dimensional anatomical surface meshes generated with the proposed mesh reduction and smoothing technique. Six reduced meshes were obtained from the original ones by merging surface vertices. The pre-defined merging distances were 0.25, 0.50, 0.75, 1.00, 1.25 and 1.50 mm. Non-shrinkage Taubin smoothing was then applied to each reduced mesh. (a) original meshes resulting from manual segmentation (upper row) and processed meshes (lower row). Overlay of original and processed meshes (right). (b) Root mean squared deviation (RMSD) of processed femur, tibia and patella meshes from their original meshes (left). A comparison of registration times observed for different mesh resolutions (right). MC25\_TAUB, for example, refers to a surface mesh smoothed with a non-shrinkage Taubin smoothing filter after a merging close surface vertices with a merging distance of 0.25 mm. (c) Evaluation of differences in transformation components (ICP registration parameters) observed with the surface meshes used in later kinematic calculation (the MC100\_TAUB version) compared to the original meshes. Evaluation on translation components ( $tx$ ,  $ty$ ,  $tz$ ) (left) and rotation components ( $ax$ ,  $ay$ ,  $az$ ,  $\theta$ ) in the axis-angle representation (right).

Figure 7(a). Bumps and steps associated with the original—manually segmented—meshes were considerably reduced. To quantify the geometric deviation of the reduced and smoothed meshes, we calculate the root mean squared deviation (RMSD) for all vertices in the processed mesh versions with reference to the original mesh. Surface meshes resulting after a mesh reduction with a 0.5 mm merging distance and a non-shrinkage Taubin smoothing fully meet the requirements in our

study as they ensure less than 0.25 mm deviation (RMSD) compared to their corresponding original meshes. Furthermore, they provide a very small to negligible overall effect on registration (less than 0.5 mm deviation in translation components (with exception of the  $z$ -component), less than 0.25 mm deviation in rotation axis and less than 0.1° deviation in rotation angle) and allow an overall registration time under 100 s for all knee components (Figure 7(b) and (c)).

**Table 3.** Overview of the anthropometric properties of the studied subjects together with the maximum flexion angle reached for each subject.

Subject ID	Gender	Measured side (L/R)	Body size (m)	Body weight (kg)	Max. flexion angle (°)
Subject 1	M	R	1.88	89	73.6
Subject 2	M	R	1.86	85	42.3
Subject 3	M	R	1.91	112	52.4
Subject 4	M	L	1.78	90	77.1
Subject 5	M	R	1.73	80	57.7
Subject 6	M	R	1.81	90	67.9
Subject 7	M	R	1.84	83	64.6
Subject 8	M	R	1.82	79	53.3
Subject 9	M	R	1.69	67	72.4
Subject 10	M	R	1.68	80	67.8



**Figure 8.** Tibiofemoral kinematics calculated using the JCS method.<sup>40</sup> Internal/external rotation, anterior/posterior translation, adduction/abduction and medial/lateral translation were calculated for the tibia with respect to the femur. (a) Tibia internal/external rotation (positive: external rotation), (b) tibia anterior/posterior translation (positive: anterior of femur), (c) tibia adduction/abduction (positive: adduction) and (d) tibia medial/lateral translation (positive: lateral of femur).

### In vivo single legged knee kinematics

Table 3 lists the maximum range of flexion achieved for all subjects together with their main anthropometric properties. Only subjects 1, 4 and 9 were able to exceed 70° flexion. Furthermore, Figure 8(a) shows—with exception for subjects 2, 4 and 10—the expected screw home motion (i.e. the internal rotation of tibia in the first 10% of extension-to-flexion). The calculated tibia's anterior/posterior translation shows persistent posterior sliding of the tibia with 12 mm in total for subject 4, Figure 8(b). Remarkable tibiofemoral kinematics could be also seen for subject 9 as well. The results show considerably large tibia motion for

internal/external rotation (3° internal rotation to 13° external rotation), for adduction/abduction (up to 12° abduction) and for medial/lateral translation (up to 11 mm medial translation).

### Discussion

Our motivation behind this work is to enhance the understanding of the complex relationship between knee anatomy and in vivo knee biomechanics. The aim of the proposed combined imaging approach is to provide a basis, which allows for the measurement of the mechanical leg axis and the assessment of knee

kinematics under physiological loading conditions in single legged stance.

General disadvantage of state-of-art approaches for in vivo knee kinematic measurement is the movement capture in atypical loading positions. In previous studies, physiological upright weight-bearing conditions could not be fully considered. Although more physiological upright loading has been achieved in two recent studies,<sup>17,37</sup> the use of inclined supporting backrests remains, however, a limitation. Previous experiments on bipedal stance kinematics are inadequate for studying physiological knee loading in daily loading conditions where the body weight is completely transferred onto one leg (e.g. during the stance phase in walking or stair climbing). Furthermore, previous in vivo kinematic studies have solely focused on the movement capture without further considerations of the mechanical leg axis. To our knowledge, the proposed MRI approach in this work is the first, which allows for the acquisition of in vivo information required for analyzing knee kinematics under full-body weight-bearing in single legged stance, and the first work that addresses the acquisition of the fully weight-bearing mechanical leg axis for the purpose of in vivo knee kinematic analysis.

Resulting internal/external rotation, anterior/posterior translation, adduction/abduction and medial/lateral translation of the tibia with respect to the femur show high discrepancy in the in vivo weight-bearing knee kinematics between the studied subjects (Figure 8). Although the studied subjects were able to achieve five increasing flexion angles, all subjects reported that the protocol took some effort. Subject 10 reported considerable muscle tremor for large flexion angles. This explains the curves outliers observed at 60° flexion for all calculated kinematics of this subject (Figure 8). Different maximum flexion angles were achieved by the individual subjects (Table 3, Figure 8). Only subjects 1, 4 and 9 were able to exceed 70° flexion. This was actually expected partly due to the different space limitations for the different subjects (subject's thigh size vs knee coil inner perimeter) but also due to the different fitness levels of the subjects. With exception for three subjects (2, 4 and 10), the expected screw home motion was observed (Figure 8(a)). In spite of the fact that the first 10% of the flexion range (flexion up to ~15°) was not directly measured in our study, the linearly interpolated curves between the first two measured tibia positions, however, reflect a clear tendency of the screw home motion. Detailed investigation of this motion necessary requires further kinematics measurements in the low flexion range. Although the exceeded posterior translation of tibia is well known in subjects suffering from a deficiency of the posterior cruciate ligament (PCL), the observed exceeded posterior tibia translation in subject 4 (up to 12 mm, Figure 8(b)) could not, however, be confirmed in this study as a consequence to a PCL deficiency as corresponding MR scans do not indicate a such deficiency in this subject. For subject 9,

the considerably large tibia motions (3° internal rotation to 13° external rotation, up to 12° abduction, up to 11 mm medial translation) may indicate high knee laxity in this subject.

Previous works on the feasibility of MRI-based determination of the mechanical leg axis were proposed by Hinterwimmer et al.<sup>49</sup> and Liodakis et al.<sup>48</sup> These two works evaluated the accuracy and reproducibility of MRI for the determination of the mechanical leg axis compared to standard X-Ray-based methods. Hinterwimmer et al.<sup>49</sup> however, compared MRI-based measurements in supine position to long radiograph-based measurements obtained in upright position and found significant underestimation for leg length and for HKA-angle in valgus knees. Liodakis et al.<sup>48</sup> however, compared HKA-angles measured from upright-MRI and weight-bearing long radiographs and found good correlation for the HKA-angle and a very high mean inter- and intra-observer agreement for the upright-MRI-based approach. However, both leg length and mechanical axis deviation (MAD) were significantly underestimated by the MRI-based technique compared to the X-Ray-based technique. In the before-mentioned two studies, MRI-based leg length measurements were evaluated against long radiographs, which are subject to systematic scaling and patient setup errors. The evaluation performed in Hinterwimmer et al.'s<sup>49</sup> study is questionable as measurements from supine MRI and bipedal stance X-Ray were compared to each other. The image acquisition protocol for length and MAD measurements in Liodakis et al.'s study used a one-coil setup and involved, therefore, coil replacements prior to knee and ankle acquisitions. Movement artifacts and patient repositioning due to coil replacements make the evaluation of mechanical leg axis, however, questionable. Another limitation of the scan protocol in Liodakis et al. is that it was not suitable for subjects taller than 1.75 m. In our work, we achieve two improvements against the before-mentioned previous works. With the developed multi-station leg scan and three coil setup, it was possible in our study to measure the mechanical leg axis in clinically applicable scan time (< 22 min—no information on required scan time was available in previous works) and without the need of coil replacement. Because no coil replacement was necessary in our approach, additional movement artifacts associated with axis measurements were, therefore, avoided. Furthermore, our optimized scan protocol provided leg axis information in subjects that stand 1.91 m high compared to maximal subject height of 1.75 m in the previous work.<sup>48</sup>

Compared to previous works, more reliable accuracy evaluation should be performed against computer tomography (CT) based measurements as CT is recognized as gold standard for length and torsion measurements.<sup>50</sup> For this purpose, ground-truth, in vitro and ex vivo CT-based measurements of the leg mechanical axis are currently being collected. Although, the planned accuracy evaluation for the mechanical leg axis will be

carried out in non-weight-bearing conditions, this will, however, be sufficient for the accuracy and reproducibility evaluation of our technique.

The proposed approach allows the non-invasive evaluation of in vivo weight-bearing knee kinematic and provides further improvements compared to previous state-of-art methods. However, the proposed method still has some limitations. Besides the high expense of MRI, the actual study protocol is demanding due to being weight-bearing at a variety of flexion angles. The total duration of the imaging technique (< 49 min for both knee flexion and leg axis acquisitions) makes the approach less feasible for assessing knee kinematics in elder and/or OA subjects. Another limitation of this approach is the acquisition of knee flexion in static postures. The recent work by D'Entremont et al.<sup>9</sup> demonstrated the utility and acceptability of dynamic MRI for knee kinematic analysis and reported differences in the three-dimensional knee kinematics obtained in dynamic MRI acquisition compared to static acquisitions. The results have been, however, obtained in 3 T scanner and in supine position. One potential future improvement to address the present limitations of our approach should include a feasibility study of dynamic acquisition techniques available on current upright-MRI systems. Future dynamic imaging protocols with substantial reduction of acquisition times would facilitate the investigations on larger population and the inclusion of subjects with less mobility and greater knee pain. However, the presented study focuses on the measurement of knee kinematics over the maximum flexion range available by the studied healthy subjects. A further adaptation for OA subjects could rather involve MR acquisitions only in the primary flexion range (up to ~30° flexion). Analysis of OA subjects could be sufficient if the quantification only focuses on the anterior and central (weight-bearing) aspects of femur with the justification that the cartilage is more frequently damaged on these aspects than the posterior aspects, and that posterior femur aspects are only in contact with tibia in large knee flexion angles.<sup>51</sup>

However, the current limited availability of upright-MRI scanners in the clinical environment remains a challenge for a future upright-MRI based investigation of loaded knee kinematics in OA subjects.

The proposed approach allows the measurement of the knee kinematics in single legged, weight-bearing flexion. This technique has been developed to measure both tibiofemoral and patellofemoral kinematics simultaneously. The focus in this work was, however, limited to the tibiofemoral kinematics. We believe that adding information from the patellofemoral kinematics along with subject-specific joint's morphology and alignment will further enhance the interpretation and discussion of the kinematics results obtained in this study. The observed kinematics discrepancy in this study underlines the need of inter-subject variability to be considered in the overall analysis. Therefore, our future work will include the development of biomechanical

simulation models with subject-specific customization capabilities to address and study the effect the subject's morphological parameters on the weight-bearing knee kinematics. The in vivo kinematic measurements obtained in this approach could be used in the validation of the computer simulation models. By addressing the previously discussed limitations of our approach, making it more feasible for OA cases, along with having validated customizable simulation models, the patient-specific preoperative planning of TKA could be further enhanced with the additionally provided functional information. In this concern, further investigations and evaluation are still required in the future.

## Acknowledgements

We would like to thank Dr Michael Schräder and the team of the clinic for Upright-Magnet Resonance Tomography in Cologne, Germany, for their support related to the optimization of the Upright-MRI protocol.

## Declaration of conflicting interests

The authors declare that there is no conflict of interest.

## Funding

This research received no specific grant from any funding agency in the public, commercial, or not-for-profit sectors.

## References

1. Statistisches Bundesamt. Fallpauschalenbezogene Krankenhausstatistik. DRG-Statistik 2012, 2012, [https://www.destatis.de/DE/Publikationen/Thematisch/Gesundheit/Krankenhaeuser/FallpauschalenKrankenhaus2120640127004.pdf?\\_\\_blob=publicationFile](https://www.destatis.de/DE/Publikationen/Thematisch/Gesundheit/Krankenhaeuser/FallpauschalenKrankenhaus2120640127004.pdf?__blob=publicationFile)
2. Delpot H, Labey L, Corte RD, et al. Collateral ligament strains during knee joint laxity evaluation before and after TKA. *Clin Biomech* 2013; 28: 777–782.
3. Hill PF, Vedi V, Williams A, et al. Tibiofemoral movement 2: the loaded and unloaded living knee studied by MRI. *J Bone Joint Surg Br* 2000; 82: 1196–1198.
4. Logan MC, Williams A, Lavelle J, et al. What really happens during the Lachman test? A dynamic MRI analysis of tibiofemoral motion. *Am J Sports Med* 2004; 32: 369–375.
5. Patel VV, Hall K, Ries M, et al. A three-dimensional MRI analysis of knee kinematics. *J Orthop Res* 2004; 22: 283–292.
6. Johal P, Williams A, Wragg P, et al. Tibio-femoral movement in the living knee. A study of weight bearing and non-weight bearing knee kinematics using “interventional” MRI. *J Biomech* 2005; 38: 269–276.
7. Williams A and Phillips C. Functional in vivo kinematic analysis of the normal knee. In Bellemans J, Ries M and Victor JM (eds) *Total knee arthroplasty*. Berlin, Heidelberg: Springer, 2005, pp.32–37.
8. Besier T, Pal S, Draper C, et al. Musculoskeletal modeling and imaging to understand patellofemoral pain. In:

- Proceedings of the International Union of Theoretical and Applied Mechanics (IUTAM) 2010*, 2010. *IUTAM Symposium on Human Movement Analysis and Simulation*, Leuven, Belgium, 13–15, September 2010. Available at: [http://www.mech.kuleuven.be/iutam2010/IUTAM\\_proceedings/abstracts\\_invitedlecturers/IUTAM\\_Besier.pdf](http://www.mech.kuleuven.be/iutam2010/IUTAM_proceedings/abstracts_invitedlecturers/IUTAM_Besier.pdf).
9. D'Entremont AG, Nordmeyer-Massner JA, Bos C, et al. Do dynamic-based MR knee kinematics methods produce the same results as static methods? *Magn Reson Med* 2013; 69: 1634–1644.
  10. Powers CM, Ward SR, Fredericson M, et al. Patellofemoral kinematics during weight-bearing and non-weight-bearing knee extension in persons with lateral subluxation of the patella: a preliminary study. *J Orthop Sports Phys Ther* 2003; 33: 677–685.
  11. Tashman S, Collon D, Anderson K, et al. Abnormal rotational knee motion during running after anterior cruciate ligament reconstruction. *Am J Sports Med* 2004; 32: 975–983.
  12. Gold GE, Besier TF, Draper CE, et al. Weight-bearing MRI of patellofemoral joint cartilage contact area. *J Magn Reson Imaging* 2004; 20: 526–530.
  13. Draper CE, Besier TF, Fredericson M, et al. Differences in patellofemoral kinematics between weight-bearing and non-weight-bearing conditions in patients with patellofemoral pain. *J Orthop Res* 2011; 29: 312–317.
  14. Scarvell JM, Smith PN, Refshauge KM, et al. Comparison of kinematics in the healthy and ACL injured knee using MRI. *J Biomech* 2005; 38: 255–262.
  15. Barrance PJ, Williams GN, Snyder-Mackler L, et al. Altered knee kinematics in ACL-deficient non-copers: a comparison using dynamic MRI. *J Orthop Res* 2006; 24: 132–140.
  16. Shin CS, Carpenter RD, Majumdar S, et al. Three-dimensional in vivo patellofemoral kinematics and contact area of anterior cruciate ligament-deficient and -reconstructed subjects using magnetic resonance imaging. *Arthroscopy* 2009; 25: 1214–1223.
  17. Nicholson JA, Sutherland AG, Smith FW, et al. Upright MRI in kinematic assessment of the ACL-deficient knee. *Knee* 2012; 19: 41–48.
  18. Carpenter RD, Majumdar S and Ma CB. Magnetic resonance imaging of 3-dimensional in vivo tibiofemoral kinematics in anterior cruciate ligament-reconstructed knees. *Arthroscopy* 2009; 25: 760–766.
  19. Vedi V, Williams A, Tennant SJ, et al. Meniscal movement. An in-vivo study using dynamic MRI. *J Bone Joint Surg Br* 1999; 81: 37–41.
  20. Yao J, Lancianese SL, Hovinga KR, et al. Magnetic resonance image analysis of meniscal translation and tibio-menisco-femoral contact in deep knee flexion. *J Orthop Res* 2008; 26: 673–684.
  21. Fellows RA, Hill NA, Macintyre NJ, et al. Repeatability of a novel technique for in vivo measurement of three-dimensional patellar tracking using magnetic resonance imaging. *J Magn Reson Imaging* 2005; 22: 145–153.
  22. Shapiro LM and Gold GE. MRI of weight bearing and movement. *Osteoarthritis Cartilage* 2012; 20: 69–78.
  23. Pappas GP, Asakawa DS, Delp SL, et al. Nonuniform shortening in the biceps brachii during elbow flexion. *J Appl Physiol* 2002; 92: 2381–2389.
  24. Asakawa DS, Blemker SS, Gold GE, et al. In vivo motion of the rectus femoris muscle after tendon transfer surgery. *J Biomech* 2002; 35: 1029–1037.
  25. Sheehan FT and Drace JE. Human patellar tendon strain. A noninvasive, in vivo study. *Clin Orthop Relat Res* 2000; 201–207.
  26. Finni T, Hodgson JA, Lai AM, et al. Muscle synergism during isometric plantarflexion in Achilles tendon rupture patients and in normal subjects revealed by velocity-encoded cine phase-contrast MRI. *Clin Biomech* 2006; 21: 67–74.
  27. Sheehan FT, Zajac FE and Drace JE. Using cine phase contrast magnetic resonance imaging to non-invasively study in vivo knee dynamics. *J Biomech* 1998; 31: 21–26.
  28. Rebmann AJ and Sheehan FT. Precise 3D skeletal kinematics using fast phase contrast magnetic resonance imaging. *J Magn Reson Imaging* 2003; 17: 206–213.
  29. Asakawa DS, Nayak KS, Blemker SS, et al. Real-time imaging of skeletal muscle velocity. *J Magn Reson Imaging* 2003; 18: 734–739.
  30. Zhu Y, Drangova M and Pelc NJ. Fourier tracking of myocardial motion using cine-PC data. *Magn Reson Med* 1996; 35: 471–480.
  31. Quick HH, Ladd ME, Hoevel M, et al. Real-time MRI of joint movement with trueFISP. *J Magn Reson Imaging* 2002; 15: 710–715.
  32. Draper CE, Santos JM, Kourtis LC, et al. Feasibility of using real-time MRI to measure joint kinematics in 1.5 T and open-bore 0.5 T systems. *J Magn Reson Imaging* 2008; 28: 158–166.
  33. Nayak KS, Cunningham CH, Santos JM, et al. Real-time cardiac MRI at 3 tesla. *Magn Reson Med* 2004; 51: 655–660.
  34. Nayak K, Hargreaves B, Besier, et al. High-Resolution Real-Time MRI of Knee Kinematics. In: *Radiological Society of North America 2003 Scientific Assembly and Annual Meeting*, 30 November–5 December 2003, Chicago IL. Available at: <http://archive.rsna.org/2003/3101925.html>. Accessed April 30, 2015.
  35. Blemker SS and McVeigh E. Real-time measurements of knee muscle moment arms during dynamic knee flexion-extension motion. In: *Proceedings of the 14th International Society for Magnetic Resonance in Medicine*, 2006, p.3619, <http://cds.ismrm.org/ismrm-2006/files/03619.pdf>
  36. Blemker SS, Asakawa DS, Gold GE, et al. Image-based musculoskeletal modeling: applications, advances, and future opportunities. *J Magn Reson Imaging* 2007; 25: 441–451.
  37. Chen B, Lambrou T, Offiah AC, et al. An in vivo subject-specific 3D functional knee joint model using combined MR imaging. *Int J Comput Assist Radiol Surg* 2013; 8: 741–750.
  38. Besier T, Draper C, Pal S, et al. Imaging and musculoskeletal modeling to investigate the mechanical etiology of patellofemoral pain. In Sanchis-Alfonso V (ed.) *Anterior knee pain and patellar instability*. London: Springer, 2011, pp.269–286.
  39. Besier T, Draper C, Pal S, et al. Imaging and musculoskeletal modeling to investigate the mechanical etiology of patellofemoral pain. In Sanchis-Alfonso V (ed.) *Atlas of the patellofemoral joint*. London: Springer, 2013, pp.125–133.
  40. Grood ES and Suntay WJ. A joint coordinate system for the clinical description of three-dimensional motions: application to the knee. *J Biomech Eng* 1983; 105: 136–144.
  41. Andersen M, Damsgaard M and Rasmussen J. Force-dependent kinematics: a new analysis method for non-

- conforming joints. In: *XIII international symposium on computer simulation in biomechanics*, Leuven, 30 June–2 July 2011.
42. Andersen M and Rasmussen J. Total knee replacement musculoskeletal model using a novel simulation method for non-conforming joints. In: *Proceedings of the International Society of Biomechanics*, Brussels, 3–7 July 2011, 343 pp. Available at: [http://isbweb.org/images/conf/2011/ScientificProgram/ISB2011\\_ScientificProgram\\_files/343.pdf](http://isbweb.org/images/conf/2011/ScientificProgram/ISB2011_ScientificProgram_files/343.pdf)
43. Taubin G. A signal processing approach to fair surface design. In: *Proceedings of the 22nd annual conference on computer graphics and interactive techniques*, Los Angeles, CA, 6–11 August 1995, pp.351–358. New York: ACM.
44. Visual Computing Lab—STI—CNR. MeshLab v1.3.2, <http://meshlab.sourceforge.net/> (accessed 3 August 2012).
45. Besl P and McKay N. A method for registration of 3-D shapes. *IEEE T Pattern Anal* 1992; 239–255.
46. Paley D, Herzenberg JE, Tetsworth K, et al. Deformity planning for frontal and sagittal plane corrective osteotomies. *Orthop Clin North Am* 1994; 25: 425–465.
47. Paley D and Pfeil J. Prinzipien der kniegelenknahen Deformitätenkorrektur. *Der Orthopäde* 2000; 29: 18–38.
48. Lioudakis E, Kenawey M, Doxastaki I, et al. Upright MRI measurement of mechanical axis and frontal plane alignment as a new technique: a comparative study with weight bearing full length radiographs. *Skeletal Radiol* 2011; 40: 885–889.
49. Hinterwimmer S, Graichen H, Vogl TJ, et al. An MRI-based technique for assessment of lower extremity deformities-reproducibility, accuracy, and clinical application. *Eur Radiol* 2008; 18: 1497–1505.
50. Keppler P, Strecker W and Kinzl L. Analyse der Beingeometrie—Standardtechniken und Normwerte. *Chirurg* 1998; 69: 1141–1152.
51. Biswal S, Hastie T, Andriacchi TP, et al. Risk factors for progressive cartilage loss in the knee: a longitudinal magnetic resonance imaging study in forty-three patients. *Arthritis Rheum* 2002; 46: 2884–2892.